Inorganica Chimica Acta xxx (2014) xxx–xxx

Contents lists available at ScienceDirect

Inorganica Chimica Acta

journal homepage: www.elsevier.com/locate/ica

Synthesis of an unsymmetrical *N*-functionalized triazacyclononane ligand and its Cu(II) complex

Mélissa Roger, Véronique Patinec *, Raphaël Tripier, Smail Triki, Nicolas Le Poul, Yves Le Mest

UMR 6521 CNRS – Université de Brest, SFR ScInBioS, UFR des Sciences et Techniques, 6 avenue Victor le Gorgeu, C.S. 93837, 29238 Brest Cedex 3, France

ARTICLE INFO

Article history:
Available online xxxx
Metals In Supramolecular Chemistry Special Issue

Keywords:
Macrocyclic ligand
Copper complex
X-ray crystal structure
Electrochemistry

ABSTRACT

The unsymmetrical 1,4-bis(2-aminophenyl)-7-(pyridin-2-ylmethyl)-1,4,7-triazacyclononane ligand (L3) has been prepared and characterized by NMR spectroscopy. The L3 ligand is based on the triazamacrocycle ring bearing one flexible 2-pyridylmethyl linked to the macrocycle group via the methyl group, and two rigid 2-aminophenyl pendant donor groups linked to the macrocycle *via* the aromatic carbon atoms. Reaction of this ligand with $Cu(ClO_4)_2{\cdot}6H_2O$ afforded the corresponding complex $[Cu(L3)](ClO_4)_2{\cdot}H_2O$ (**4**) which was structurally characterized both in solid state and in solution. The crystal structure of **4** consists of a discrete monomeric $[Cu(L3)]^{2+}$ in which the Cu(II) ion is six coordinated with three nitrogen atoms of the macrocycle ring, two of the aminophenyle and one of the pyridine appended functions. The triazacyclonane macrocycle ring is facially coordinated and the *N*-donor atoms of the three pendant groups (two aniline and one pyridine groups), are disposed in the same side of the basal macrocyclic ring, leading to a distorted and elongated CuN_4N_2 octahedron. UV–Vis spectroscopy of complex **4** in acetonitrile displays a d–d transition band at $\lambda = 673$ nm. The voltammetric studies show that the $[Cu(L3)]^{2+}$ cation can be reduced quasi-reversibly and oxidized irreversibly, both process being monoelectronic.

1. Introduction

More and more attentions are being attracted by the research on copper metal complexes due to their implications in many different domains, such as nuclear medicine for imaging diagnosis (PET) and radioimmunotherapy (RIT) [1,2], biochemistry for mimicking active sites of metalloenzymes [3–8], sensing for cation detection [9–12]. These various applications usually necessitate the design and tailoring of ligands which fit at best in the requirements. The polyazacycloalkane ligands such as tacn (1,4,7-triazacyclononane) are very much investigated in these different research fields owing to their ability to form very stable complexes with transition metals cations [13–15] and their possible easy transformation by *C*- or *N*-functionalization of the macrocyclic platform [16,17]. The small azamacrocycle tacn is known for coordinating transition metals as copper (II) in a facial manner, with the cation located above the plane formed by the three nitrogen atoms of the cycle. Additional pendant arms containing donor atoms on the triamine macrocycle complete the coordination sphere of the cation leading to the high stability of the complexes [13–15]. Configurational environment of the ligand around the transition metal ion depends strongly on the geometry and on these pendant arms. Therefore, such *N*-functionalized groups impact on the cation coordination sphere nature and geometry and, then on the complex properties. Among the already described $[CuN_6]$ tacn complexes, two complexes exhibiting five-membered chelate rings, caught our attention regarding the flexibility degree of the triazamacrocyclic coordinating arms. The first one is based on the macrocycle ligand bearing three flexible 2-pyridylmethyl which are linked to the N_3-macrocycle group *via* methylene groups (L1) [18,19]; the second one is based on the macrocycle ligand involving three rigid 2-aminophenyl pendant donor groups, linked to the macrocycle group *via* the aromatic carbon atoms (L2) [20] (Scheme 1).

Herein, we report the synthesis and characterization of the intermediary system based on unsymmetrical 1,4,7-triazacyclononane (L3) and of its Cu(II) complex $[Cu(L3)](ClO_4)_2{\cdot}H_2O$ (**4**), including its spectroscopic and electrochemical properties.

2. Experimental

2.1. Reagents and techniques

Solvents and reagents were obtained from commercial suppliers, and were used without further purification. Starting tacn was

* Corresponding author. Tel.: +33 298017927; fax: +33 298017001.
E-mail address: veronique.patinec@univ-brest.fr (V. Patinec).

http://dx.doi.org/10.1016/j.ica.2013.12.036
0020-1693/

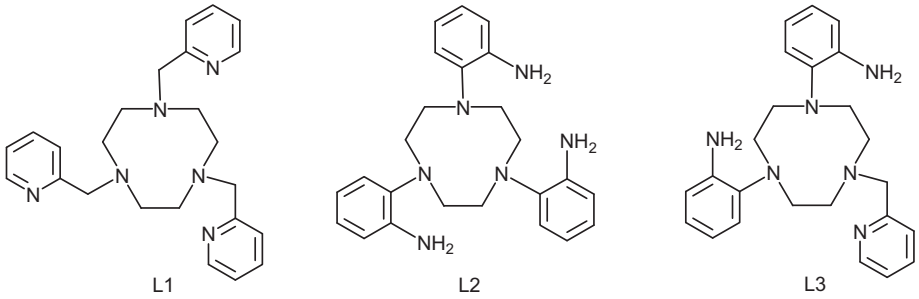

Scheme 1. Ligands discussed in this paper.

purchased from CheMaTech (Dijon, France). Elemental analyses were performed by the "Service Central d'Analyses du CNRS", Gif-sur-Yvette, France. Infrared spectra were recorded in the range 4000–200 cm^{-1} on a FT-IR BRUKER ATR VERTEX70 Spectrometer. Diffraction analyses were performed using an Oxford Diffraction Xcalibur -CCD diffractometer. NMR and MALDI mass spectra were carried out by the "Services communs" of the University of Brest. MALDI mass spectra were recorded with an Autoflex MALDI TOF III LRF200 CID spectrometer. NMR spectra were recorded on a Brucker Avance 400 (400 MHz) or a Bruker AMX-3 300 (300 MHz). UV–Vis–NIR spectroscopy was performed with a JASCO V-670 spectrophotometer with a classical cell holder. The electrochemical studies in acetonitrile were performed in a glovebox (Jacomex) (O_2 <1 ppm, H_2O <1 ppm) with a home-designed 3-electrodes cell (WE: vitreous carbon electrode, RE: Pt wire in a solution of CH_3CN/NBu_4PF_6 containing equimolar amounts of ferrocene and ferrocenium hexafluorophosphate, CE: Pt). Acetonitrile (CH_3CN) (99.9% BDH, VWR) was distilled over CaH_2 and stored after freeze-pumping in the glovebox under argon. NBu_4PF_6 was synthesized from NBu_4OH (Fluka) and HPF_6 (Aldrich). It was then purified, dried under vacuum for 48 h at 100 °C, then kept under N_2 in the glovebox. The potential of the cell was controlled by an AUTOLAB PGSTAT 302 (Ecochemie) potentiostat monitored by a computer. Ferrocene (Fc) was added at the end of each experiment to determine accurate redox potential values.

Cautions! Perchlorate salts of metal complexes are potentially explosive and should be handled with care in small quantities.

2.2. Synthetic procedures

2.2.1. Synthesis of 1,4-bis(2-aminophenyl)-7-(pyridin-2-ylmethyl)-1,4,7-triazacyclononane (*L3*)

*2.2.1.1. Preparation of 10-phenyl-1,4,7-triazabicyclo[5.2.1] decane (**1**).* 5 mmol of 1,4,7-triazacyclononane (645 mg) and benzaldehyde (508 μL, 5 mmol) were stirred at room temperature in distilled ethanol (80 mL) containing molecular sieve for 4 h. The solution was filtered and evaporated under reduced pressure to yield the aminal product as a white solid (980 mg, 4.5 mmol, 90%). NMR ($CDCl_3$) ^1H (300 MHz) 2.89–2.93 (m, 4H,CH_{2tacn}) 2.99–3.03 (m, 2H,CH_{2tacn}) 3.07–3.17 (m, 4H,CH_{2tacn}) 3.32–3.39 (m, 2H,CH_{2tacn}) 5.66 (s, 1H, H_{aminal}) 7.18 (t, 1H, H_{Phe}) 7.29 (t, 2H, H_{Phe}) 7.50 (2H, d, H_{Phe}); ^{13}C (75 MHz) 49.3 49.6 58.8 (CH_{2tacn}) 88.3 (C_{aminal}) 126.6, 126.7 128.2 (CH_{Phe}) 145.8 (C_{Phe}).

*2.2.1.2. Preparation of 1-(pyridin-2-ylmethyl)-1,4,7-triazacyclononane (**2**).* 10-phenyl-1,4,7-triazabicyclo[5.2.1] decane (1) (4.5 mmol, 980 mg) and 575 mg of 2-methylpyridine chloride (4.5 mmol) were stirred with potassium carbonate (3 g, excess) in distilled acetonitrile at room temperature for 4 days. Filtration and solvant elimination gave a brown oily product. After hydrolysis in HCl 1 M (15 mL) at room temperature for 3 h, extraction at pH1 with $CHCl_3$ (2 × 20 mL) allowed to eliminate traces of organic impurities. The aqueous solution was made basic (pH >12) with NaOH pellets and extracted with $CHCl_3$ (3 × 20 mL), dried over $MgSO_4$, filtered and the solvant evaporated to yield the compound (2) as a coloured oil (740 mg, 75%). NMR ($CDCl_3$, 300 MHz) ^1H 2.44–2.45 (m, 8H, CH_{2tacn}) 2.56–2.58 (m, 4H, CH_{2tacn}) 3.11 (bs, 2H, N*H*) 3.65 (s, 2H, CH_{2pyr}) 6.89 (m, 1H, CH_{pyr}) 7.17 (m, 1H, CH_{pyr}) 7.39 (m, 1H, CH_{pyr}) 8.28 (m, 1H, CH_{pyr}); ^{13}C ($CDCl_3$, 75 MHz) 45.9 46.3 52.4 (CH_{2tacn}) 61.6 (CH_{2pyr}) 121.5 122.5 135.9 148.5 (CH_{pyr}) 159.3 (C_{pyr}).

*2.2.1.3. Preparation of 1,4-bis(2-nitrophenyl)-7-(pyridin-2-ylmethyl)-1,4,7-triazacyclononane (**3**).* 1-fluoro-2-nitrobenzene (370 μL, 3.5 mmol) was added to 355 mg of 1-(pyridin-2-ylmethyl)-1,4,7-triazacyclononane (1.6 mmol) and an excess of potassium carbonate (1.10 g, 8.0 mmol (5 eq)) in distilled acetonitrile (20 mL). The reaction mixture was stirred at reflux under nitrogen atmosphere during 12 h. The hot solution was filtrated and the filtrate evaporated under reduced pressure. The residue was purified by silica gel chromatography (Hexane then Hexane/$CHCl_3$:1/1) to yield an orange oil (690 mg, 93%). NMR ($CDCl_3$, 300 MHz) ^1H 2.89 (m, 4H, CH_{2tacn}) 3.35 (m, 4H, CH_{2tacn}) 3.68 (bs, 4H, CH_{2tacn}) 3.77 (s, 2H, CH_{2pyr}) 6.81 (t, 2H, CH_{Phe}) 7.00 (d, 2H, CH_{Phe}) 7.08 (t, 1H, CH_{pyr}) 7.34 (m, 3H, CH_{Phe} + CH_{pyr}) 7.53 (t, 1H, CH_{pyr}) 7.59 (dd, 2H, CH_{Phe}) 8.44 (d, 1H, CH_{pyr}); ^{13}C ($CDCl_3$, 75 MHz) 53.8 54.5 55.1 (CH_{2tacn}) 64.2 (CH_{2pyr}) 118.6 119.4 (CH_{Phe}) 121.9 123.3 (CH_{pyr}) 126.1 132.8 (CH_{Phe}) 136.2 (CH_{pyr})141.1 143.7(*C*) 148.8 (CH_{pyr})159.1(*C*); MALDI-TOF: *m*/*z* 463.2 [M+1$^+$].

2.2.1.4. Preparation of 1,4-bis(2-aminophenyl)-7-(pyridin-2-ylmethyl)-1,4,7-triazacyclononane (L3). 1,4-bis(2-nitrophenyl)-7-(pyridin-2-ylmethyl)-1,4,7-triazacyclononane (325 mg, 0.80 mmol) in absolute ethanol (30 mL) was stirred at reflux under nitrogen atmosphere during 3 days with 10 mL (excess) of hydrazine monohydrate and activated carbon. After cooling, the solution was filtrated and the filtrate was evaporated under reduced pressure. The residue was dissolved in $CHCl_3$ (20 mL) and $MgSO_4$ was added. After filtration, elimination of the solvent under reduced pressure yielded the product as a brown oil (205 mg, 73%). NMR ($CDCl_3$, 400 MHz) ^1H 2.99–3.02 (m, CH_{2tacn}, 4H) 3.29–3.31 (m, CH_{2tacn}, 4H) 3.35 (s, CH_{2tacn}, 4H) 3.94 (s, CH_{2pyr}, 2H) 6.65–6.72 (m, 4H, CH_{Phe}) 6.89 (t, 2H, CH_{Phe}) 7.07 (d, 2H, CH_{Phe}) 7.18 (t, 1H, CH_{pyr}) 7.46 (d, 1H, CH_{pyr}) 7.67 (t, 1H, CH_{pyr}) 8.56 (d, 1H, CH_{pyr}); ^{13}C ($CDCl_3$, 100 MHz) 55.8 56.0 56.7 (CH_{2tacn}) 64.9 (CH_{2pyr}) 115.4 118.2 (CH_{Phe}) 122.0 (CH_{pyr}) 123.3 (CH_{Phe}) 123.4 (CH_{pyr}) 124.4 (CH_{Phe}) 136.3 (CH_{pyr}) 140.9 142.7 (*C*) 149.1 (CH_{pyr}) 159.4 (*C*); MALDI-TOF: *m*/*z* 403.2 [M+1$^+$].

2.2.2. Synthesis of $[Cu(L3)](ClO_4)_2{\cdot}H_2O$ (*4*) complex

An aqueous solution (5 mL) of L3 (0.05 mmol, 20.13 mg) was added progressively, under continuous stirring, to an aqueous solution (10 mL) of $Cu(ClO_4)_2{\cdot}6H_2O$ (0.05 mmol, 18.53 mg). Slow

evaporation of the resulting blue solution gave blue crystals of **4**. Yield: 24.2 mg, 71.0%. *Anal.* Calc. for $C_{24}H_{32}Cl_2CuN_6O_9$: C, 42.2; H, 4.7; N, 12.3. Found: C, 41.9; H, 4.8; N, 12.5%. IR (cm^{-1}): 3267(br), 3169(br), 1614(m), 1570(m), 1496(m), 1481(m), 1456(m), 1366(w), 1278(w), 1228(w), 1061(s), 1012(w), 924(w), 830(m), 810(m), 766 (w), 741(w), 618(s), 559(w), 532(w), 458(w). Single crystals of **4** were used for crystallographic study and for the preparation of an acetonitrile solution of **4** to perform UV–Vis spectroscopic and electrochemical studies.

2.3. X-ray crystallography

Crystallographic study of **4** was performed at 170 K, using an Oxford Diffraction Xcalibur κ-CCD diffractometer equipped with a graphite monochromated Mo Kα radiation (λ = 0.71073 Å). The full sphere data collections were performed using 1.0° -scans with an exposure time of 60 s per frame. Data collection and data reduction were done with the CRYSALIS-CCD and CRYSALIS-RED programs on the full set of data [21,22]. The crystal structures were solved by direct methods and successive Fourier difference syntheses, and were refined on F^2 by weighted anisotropic full-matrix least-square methods [23]. All non-hydrogen atoms were refined anisotropically, while the hydrogen atoms were calculated and therefore included as isotropic fixed contributors to F_c. All other calculations were performed with standard procedures (WINGX) [24]. Crystal data, structure refinement and collection parameters are listed in Table 1.

Table 1
Crystal data and structural refinement parameters for $[Cu(L3)](ClO_4)_2{\cdot}H_2O$ (4).

Empirical formula	$C_{24}H_{32}Cl_2CuN_6O_9$
Molecular weight	683.00
Space group	$P2_1/n$
a (Å)	10.6442(3)
b (Å)	16.4183(5)
c (Å)	16.6388(5)
β (°)	93.255(3)
V (Å^3)	2903.1(2)
Z	4
ρ_{calc} (g cm^{-3})	1.563
μ (cm^{-1})	9.98
$F(000)$	1412
Reflections measured	23 005
2θ range (°)	5.54–54.00
Reflections unique (R_{int})	6318/0.0639
Reflections with $I > 2\sigma(I)$	3799
N_v	379
[a]R_1/[b]wR_2	0.0471/0.1174
[c]Goodness-of-fit (GOF)	0.976
$\Delta\rho_{max,min}$ (e Å^{-3})	+0.601, −0.353

[a] $R1 = \sum|F_o - F_c|/F_o$.
[b] $wR_2 = \{\sum[w(F_o^2 - F_c^2)^2]/\sum[w(F_o^2)^2]\}^{1/2}$.
[c] $GOF = \{\sum[w(F_o^2 - F_c^2)^2]/(N_{obs} - N_{var})\}^{1/2}$.

2.4. Solution studies

Spectroscopic and electrochemical studies were performed using acetonitrile solution of single crystals of **4** (0.8 mM) containing electrolyte salt (NBu_4PF_6 0.1 M).

3. Results and discussion

3.1. Synthesis

The strategy used for L3 synthesis is based on the initial formation of 1-(pyridine-2-ylmethyl)-1,4,7-triazacyclononane (2) followed by the introduction of two reductible 2-nitrophenyl arms on the remaining secondary amine functions of the triazamacrocycle. 1-(pyridin-2-ylmethyl)-1,4,7-triazacyclononane (2) has been synthesised by exploiting the aminal protection route [25]: reaction of tacn with benzaldehyde allowed the formation of 10-phenyl-1,4,7-triazabicyclo[5.2.1] decane (1) leaving one secondary amine function free to react with 2-methylpyridine chloride according to a nucleophilic substitution. Acidic hydrolysis of the corresponding product 4-(pyridin-2-ylmethyl)-10-phenyl-1,4,7-triazabi-cyclo[5.2.1] decane with HCl 1 M allowed to recover the 1-(2-pyridylmethyl)(tacn) (2). The reaction of (2) with two equivalents of 1-fluoro-2-nitrobenzene gave easily the tacn derivative bearing two 2-nitrophenyl and one 2-pyridylmethyl arms (3) with a very good yield (93%). Reduction of nitro into amino groups was carried out by hydrazine hydrate in ethanol giving the ligand L3 with good yield (73%) (Scheme 2). NMR characterization and mass spectroscopy are in fully accordance with L3 structure.

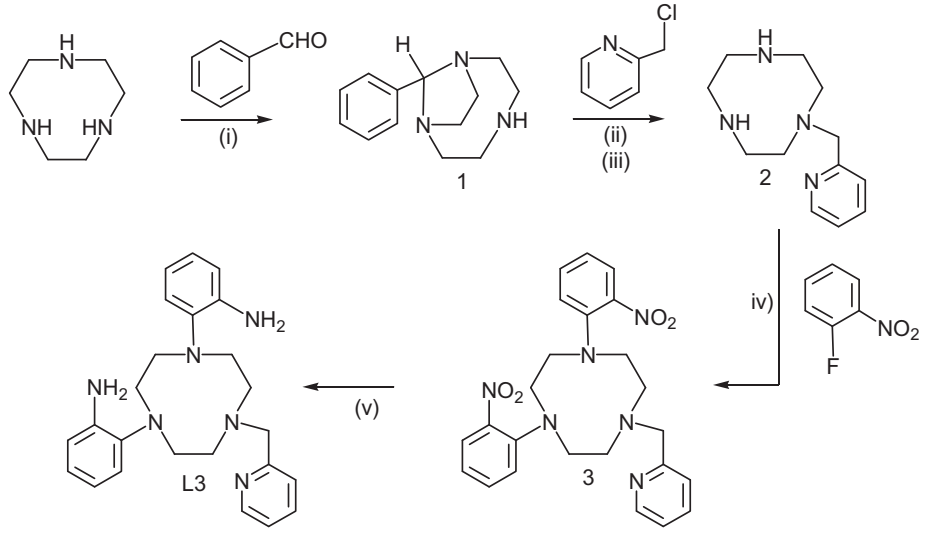

Scheme 2. Five steps synthesis of ligand L3. (i) Ethanol, molecular sieve, RT, 4 h; (ii) CH_3CN, K_2CO_3, RT, 4 days; (iii) HCl 1 M, RT, 3 h/OH^-; (iv) CH_3CN, K_2CO_3, Δ, 12 h under N_2; (v) NH_2NH_2, H_2O/ethanol, activated carbon, Δ, 3 days under N_2.

Table 2
Selected bond distances (Å) and bon angles (°) for complex **4**.

Cu–N1	2.287(3)	Cu–N4	2.095(3)
Cu–N2	2.095(3)	Cu–N5	1.998(3)
Cu–N3	2.055(3)	Cu–N6	2.258(3)
N1–Cu–N2	82.17(10)	N2–Cu–N6	96.44(11)
N1–Cu–N3	81.78(10)	N3–Cu–N4	98.31(11)
N1–Cu–N4	79.33(10)	N3–Cu–N5	168.21(11)
N1–Cu–N5	102.07(11)	N3–Cu–N6	79.13(11)
N1–Cu–N6	160.90(10)	N4–Cu–N5	93.37(11)
N2–Cu–N3	85.00(11)	N4–Cu–N6	103.06(11)
N2–Cu–N4	160.50(11)	N5–Cu–N6	96.72(12)
N2–Cu–N5	84.51(11)		

3.2. Crystal structure description

Single crystals of **4** were obtained by slow evaporation of an aqueous solution containing triazamacrocyclic ligand (**L3**) and $Cu(ClO_4)_2$ in a 1/1 ratio. The $[Cu(L3)](ClO_4)_2{\cdot}H_2O$ (**4**) complex crystallizes in the monoclinic $P2_1/n$ space group. The unit cell parameters, crystal and refinement data, and the pertinent bond distances and bond angles are summarized in Tables 1 and 2, respectively.

The crystal structure consists of a discrete monomeric $[Cu(L3)]^{2+}$ cation (Fig. 1), two uncoordinated perchlorate anions and one water molecule. The Cu(II) ion is six coordinated with three nitrogen atoms of the macrocycle (N1, N2 and N3), two of the phenylamine rings (N4 and N5) and one of the pyridine ring (N6). Examination of the six Cu–N bonds allows us to describe the metal environment as a distorted and elongated CuN_4N_2 octahedron. The two apical positions (Cu–N1: Cu–N1: 2.287(3) Å; Cu–N6: 2.258(3) Å) are occupied by one nitrogen atom belonging to the macrocycle (N1) and one nitrogen atom (N6) of the 2-pyridylmethyl pendant arm; while the equatorial plane involves two short (Cu–N3 and Cu–N5: 2.055(3) and 1.998(3) Å, respectively) and two equivalent intermediate Cu–N (Cu–N2 and Cu–N4: 2.095(3) Å) distances.

As observed in other similar tacn N-functionalized macrocycle ligands (L1 et L2) [18–20], the macrocycle is facially coordinated and the N-donor atoms of the three pendant groups (two aniline and one pyridine groups), are disposed in the same side of the basal macrocyclic ring. This fact results from the relatively small size of the tacn ring forcing the metal ion to remain well above the mean ring plane. The distance of the Cu(II) metal ion to the perfect plane generated by the three nitrogen atoms of the macrocycle ring (N1, N2 and N3) is 1.37 Å.

Reports based on the parent Cu(II) discrete complexes involving the tacn ring with similar pendant arms, reveal only two examples: $[(CuL1)_2](ClO_4)_4$ (**5**) [18,19] and $[CuL2](ClO_4)_2$ (**6**) [20]; where L1 ligand involves three flexible 2-pyridylmethyl pendant arms, while L2 ligand involves three rigid 2-aminophenyl pendant groups (see Scheme 1). Both complexes **5** and **6** have been reported as exhibiting discrete structures [18–20]. However a perusal of the data for the metal environments in the two complexes (Table 3) reveals that they differ strongly by their metal environments: the asymmetric unit of **5** consists of two different $[CuL1]^{2+}$ cations; the first one displays a regular elongated CuN_4N_2 octahedron, with two long axial distances (2.192(8) and 2.198(8) Å) and four shorter equatorial distances in the range 2.080–2.138 Å (see column 1 in Table 3), nearly similar to that described for complex **4**. However, the second Cu(II) environment of **5** and that of complex **6** can be viewed as CuN_3N_3 distorted octahedrons, since their corresponding

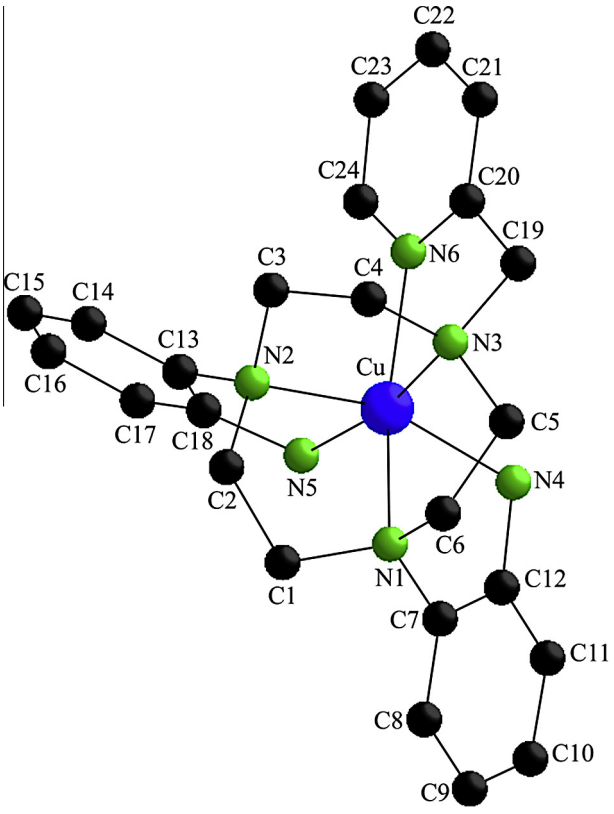

Fig. 1. Structure of cationic complex of **4** showing the atom labelling scheme and the coordination environment of the Cu(II) ion (N1 and N6 are the two apical positions of the elongated CuN_4N_2 octahedron).

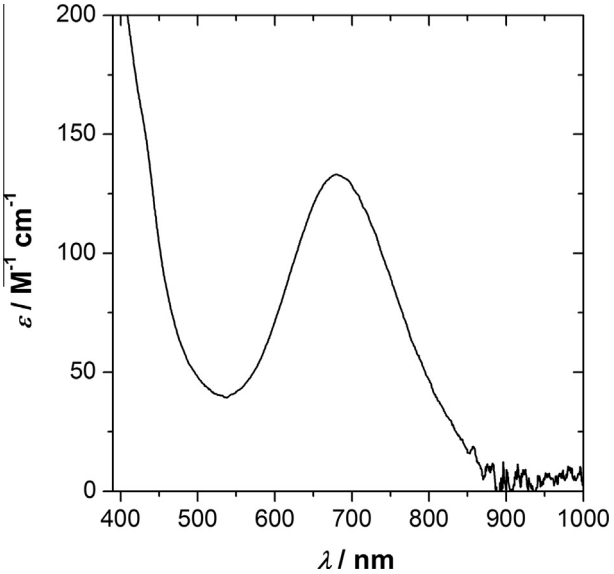

Fig. 2. UV–Vis spectrum of complex **4** (0.8 mM) in CH_3CN/NBu_4F_6 (0.1 M).

Table 3
Cu–N distance in Cu(II) tacn N-functionalized macrocycle based complexes.

	5		**6**	**4**
Cu–N(amine)	2.110(8)	2.041(8)	2.024(9)	2.055(3)
	2.111(8)	2.180(8)	2.193(8)	2.095(3)
	2.192(8)	2.239(9)	2.218(9)	2.287(3)
Cu–N(py)	2.080(8)	1.995(8)		–
	2.138(8)	2.115(8)		–
	2.198(8)	2.211(9)		2.258(3)
Cu–N(aniline)			2.032(8)	1.998(3)
			2.081(9)	2.095(3)
			2.211(9)	–
References	[18,19]		[20]	This work

Table 4
UV–Vis and electrochemical data for complex **4** and analogous Cu complexes in CH_3CN/NBu_4PF_6.

Complex	λ_{max} (nm) (ε_{max} (M^{-1} cm^{-1}))	$E^0(1)$/V vs. F_c	Refs.
4	683 (110)	−0.71	This work
[Cu(dmptacn)] $(ClO_4)_2$	612 (210)[a]	−0.81[b]	[26]
5	693 ([c])[a]	[c]	[18]
6	695 (107)[a]	[c]	[20]
[Cu($(BzNH_2)_3$tacn)] $(ClO_4)_2$	605 (276)[a]	[c]	[27]
[Cu(iPr_3tacn)($CH_3CN)_2$] $(SbF_6)_2$	669 (170)[d]	−0.04[e,f]	[28,29]

[a] Measured in CH_3CN.
[b] Measured in CH_3CN/NBu_4ClO_4.
[c] Not determined.
[d] In CH_2Cl_2.
[e] Assuming $E^0(F_c^+/F_c)$ = +0.40 V vs. SCE.
[f] Data determined from Cu(I) complex.

crystallographic data reveals, in each case, two axial and one equatorial Cu-N distances, much more longer than the three other ones (see columns 2 and 3 in Table 3), giving rise to a meridional (*mer*) configuration.

3.3. Solution studies

The spectroscopic and electrochemical properties of the complex **4** were investigated in acetonitrile containing electrolyte salt (NBu_4PF_6 0.1 M) at room temperature. The UV–Vis spectrum of the complex displays an absorption band at λ = 683 nm (ε = 110 M^{-1} cm^{-1}) (Fig. 2). The band at 683 nm can be ascribed to a d-d transition as classically observed for Cu(II) complexes. This wavelength value is close to that found for analogous complexes in the same solvents (Table 4). It confirms the tetragonal character of the N-based coordination sphere surrounding the cupric ion, in agreement with the solid state structure.

Voltammetric studies in CH_3CN/NBu_4PF_6 at a vitreous carbon electrode were performed to rationalize the effect of the L3 ligand on the coordination of the Cu(II) ion, in comparison to existing data. Fig. 3A displays the cyclic voltammetric behaviour of the complex when scanning negatively until −2.1 V versus F_c (plain line).

Two reduction peaks were detected at ca −0.8 V and −1.0 V and the backscan of the more negative process indicated a Cu(0) anodic redissolution peak (peak *, Fig. 3A), as typically observed for Cu(I) complexes upon reduction. This oxidation peak disappeared when

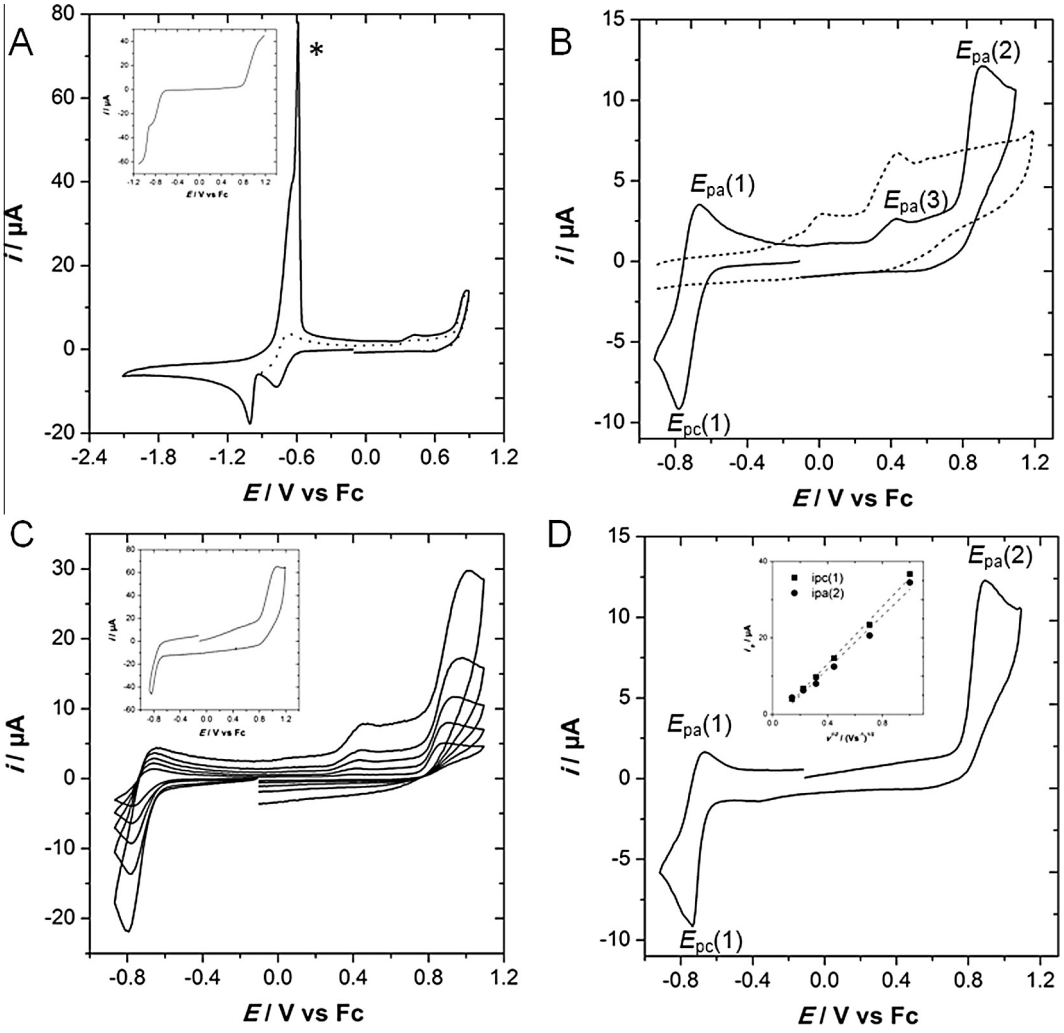

Fig. 3. Voltammetry at a vitreous carbon electrode in CH_3CN/NBu_4PF_6 0.1 M (E/V vs. F_c): (A) Complex **4** (0.8 mM) (v = 0.1 V s^{-1}) with first vertex potential at −2.1 V (plain line) and −0.9 V (dotted line); peak * corresponds to Cu^0 redissolution; inset: Rotating-Disk Electrode Voltammogram (1000 t min^{-1}); (B) Complex 4 (0.8 mM) (plain line) with negative initial scan (v = 0.1 V s^{-1}) and ligand L3 (0.5 mM) (dotted line) with positive scan; (C) Complex **4** (0.8 mM) for 0.02 V s^{-1} < v < 0.5 V s^{-1} with negative initial scan, inset (v = 5 V s^{-1}); (D) Complex **4** (0.8 mM) (v = 0.1 V s^{-1}) with positive initial scan. Inset: plots of $|i_{pc}(1)|$ and $i_{pa}(2)$ vs. $v^{1/2}$.

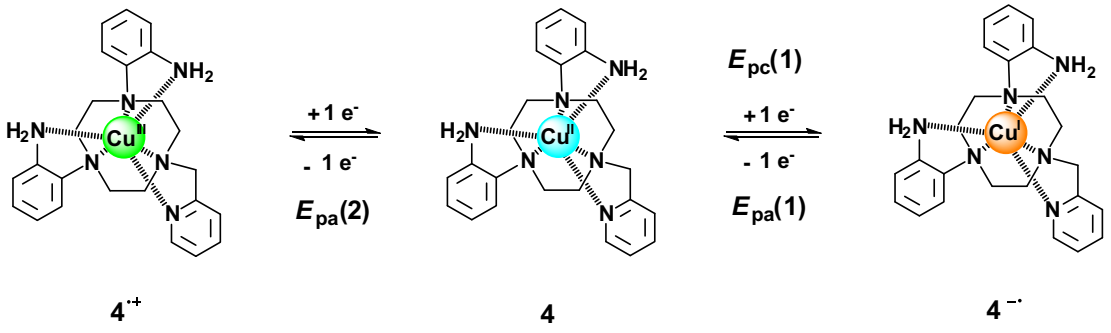

Scheme 3. Proposed-redox processes for complex **4**.

reversing the scan at potential values (E) higher than −0.9 V (Fig. 3A, dotted line). For −1.2 V < E < 1.3 V, rotating-disk electrode voltammetry (RDEV) displayed two reduction and one oxidation waves of almost equal current intensities (inset Fig. 3A). By correlation with cyclic voltammetric results, the two reduction waves are ascribed to the Cu(II)/Cu(I) and Cu(I)/Cu(0) processes (the higher slope of the wave for the second process supports the formation of Cu(0) onto the electrode surface). On this basis, we restricted our voltammetric studies on complex 4 and ligand L3 to potential values higher than −0.9 V. As depicted in Fig. 3B, the complex 4 (plain line) shows a quasi-reversible system at $E^{0\prime}(1)$ = −0.71 V versus F_c ($\Delta E_p(1) = E_{pa}(1) - E_{pc}(1)$ = 110 mV), and two irreversible oxidation peaks on the back scan at $E_{pa}(2)$ = +0.93 V and $E_{pa}(3)$ = +0.43 V when starting negatively from the zero-current potential (0 V). When starting positively (Fig. 3D), the oxidation peak at $E_{pa}(3)$ disappeared while the systems (1) and (2) remained present. On the other hand, the free ligand L3 showed two irreversible oxidation peaks at 0.01 V and 0.43 V when scanning positively from −0.90 V (Fig. 3B, dashed line). At last, the increase of the scan rate (0.02 V s^{-1} < v < 5 V s^{-1}) induced the decrease of intensity of the peak at $E_{pa}(1)$ whereas the irreversible peak at $E_{pa}(3)$ increased and the peak at $E_{pa}(2)$ remained present (Fig. 3C). At v = 5 V s^{-1} (inset Fig. 3C), total irreversibility was detected for $E_{pc}(1)$. Exhaustive electrolysis of the solution at E = −0.9 V on a graphite rod led to the deposition of Cu on the electrode surface. The resulting RDEV and CV showed the presence of the three systems at $E^{0\prime}(1)$, $E_{pa}(2)$ and $E_{pa}(3)$ with predominance of the system at $E_{pa}(3)$. Exhaustive electrolysis of the initial solution at E = 1.0 V lead to disappearance of all systems.

RDEV and CV data show clearly that two redox processes can be assigned to the complex 4: Cu(II)/Cu(I) for the reduction at $E_{pc}(1)$ and Cu(III)/Cu(II) for the oxidation at $E_{pa}(2)$. This is inferred for the latter as the similar peak heights imply that electronic transfer involves the same number of charge in each process (insets Fig. 3A and Scheme 3). This proposal is in agreement with previous electrochemical analysis of $[Cu(dmptacn)]^{2+}$ (two picolyl groups and three amino from the tacn core) [26]. The CV behaviour of complex 4 indicates that both amino moieties are coordinated to the Cu(II) ion as no free amine oxidation peaks are observed, (Fig. 3B and 3D). This is also supported by the fact that the $E^{0\prime}(1)$ value for 4 is much lower than that obtained for the $[Cu(iPr_3tacn)]^+$ complex and similar to that found for the five-coordinated $[Cu(dmptacn)]^{2+}$ complex (Table 4).

Focusing now on the reduction process occurring at $E_{pc}(1)$, CV shows that the electrogenerated Cu(I) complex is not stable under these experimental conditions and evolves rapidly towards a new species which displays an oxidation potential peak at $E_{pa}(3)$. This new species only results from the reduction of the initial Cu(II) complex since the peak at $E_{pa}(3)$ does not appear when scanning positively (Fig. 3D). Moreover, the relative intensities of peaks at $E_{pa}(1)$ and $E_{pa}(3)$ are correlated with the variation of the scan rate. Such behaviour is indicative of a chemical equilibrium involving two oxidizable species. This is frequently observed for Cu(II)/Cu(I) systems as associated with the geometric reorganization between each redox state (five- or six-coordinate for Cu(II) against four-coordinate for Cu(I)) [30].

In the present case, conformational changes may be related to the decoordination of one or two coordinating amino arms by reduction at the Cu(I) state, as previously observed for analogous complexes [31–33]. As when v is increased, the $i_{pa}(3)/i_{pa}(1)$ ratio is also increased, shown by CV at variable scan rates (Fig. 3C), the forward chemical reaction (decoordination) which follows the electrochemical reduction would be faster than the backward reaction (re-binding of the arm(s)). These processes are under investigation for a full understanding of the mechanism.

Another interesting information which is given by voltammetry is the irreversible oxidation process occurring at $E_{pa}(2)$. As already mentioned the good match between peak heights at various scan rates for the systems (1) and (2) suggests that the oxidation is monoelectronic (Scheme 3). In each case, plots of $i_{pa}(2)$ and $i_{pc}(1)$ versus $v^{1/2}$ yield a linear slope as expected for a diffusion-limited process (inset Fig. 3D). The detection of Cu(III) species by electrochemistry has been mainly reported for N/O macrocyclic systems appending strong donating ligands [31–33]. In the present example, the oxidation potential is relatively high in comparison to these systems in analogous conditions. Interestingly, the energy gap between $E_{pa}(2)$ and $E_{pc}(1)$ (ca 1.8 V) is relatively low compared to existing data (typically ΔE > 2 V [34–38]). This effect may result from the constraint exerted by the short spacer between the aniline moiety and the tacn core which destabilizes the Cu(II) redox state and favours high reduction and low oxidation potentials.

4. Conclusions

The new functionalized 1,4-bis(2-aminophenyl)-7-(pyridin-2-ylmethyl)-1,4,7-triazacyclononane ligand (L3) has been synthesized using the aminal route for specifically grafting one 2-pyridylmethyl arm and then two aniline groups on the tacn core. Its corresponding Cu(II) complex, $[Cu(L3)](ClO_4)_2{\cdot}H_2O$ (**4**), has been prepared and structurally characterized. As the parent complexes previously reported, the $[Cu(L3)]^{2+}$ complex displays a discrete monomeric $[Cu(L3)]^{2+}$ in which the macrocycle ring is facially coordinated and the N-donor atoms of the three pendant groups (two aniline and one pyridine groups), are disposed on the same side of the basal macrocyclic ring. However, complex **4** exhibits a regular elongated CuN_4N_2 octahedron different from the two Cu(II) complexes based on symmetrically functionalized tacn ligand (see L1 and L2 ligands in Scheme 1) for which the metal environment displays a CuN_3N_3 distorted geometry, close to a meridional (*mer*) configuration. In addition to the nature of the metal ion, this

coordination versatility can be attributed to the flexibility of the macrocycle ring despite the presence of the rigid 2-aminophenyl pendant donor groups. The electrochemical study showed that the $[Cu(L3)]^{2+}$ complex can be reduced quasi-reversibly and oxidized irreversibly, both process being monoelectronic.

Acknowledgments

The authors acknowledge the CNRS (“Centre National de la Recherche Scientifique”), the Brest University, the french “Ministère de l’Enseignement Supérieur et de la Recherche”, the “Ministère des Affaires Etrangères et Européennes” (PHC Maghreb project No. 30255ZJ) and the “Agence Nationale de la Recherche” (ANR project BISTA-MAT: ANR-12-BS07-0030-01). Authors especially thank the financial support from the Région Bretagne, France and also the “Service Commun” of NMR facilities of the University of Brest.

Appendix A. Supplementary material

NMR spectra (^{1}H, ^{13}C) of L3 ligand are provided in supplementary data. Crystallographic data have been deposited in the Cambridge Crystallographic Data Centre under the CCDC number 958291 that contains the supplementary crystallographic data for compound **4**. These data can be obtained free of charge *via* the web application at www.ccdc.cam.ac.uk/conts/retrieving.html [or from the Cambridge Crystallographic Data Center, 12 Union Road, Cambridge CB2 1EZ, UK: Fax: +44 1223 336 033; E-mail: deposit@ccdc.cam.ac.uk]. Supplementary data associated with this article can be found, in the online version, at http://dx.doi.org/10.1016/j.ica.2013.12.036.

References

[1] S.V. Smith, J. Inorg. Biochem. 98 (2004) 1874.
[2] M. Shokeen, C.J. Anderson, Acc. Chem. Res. 42 (2009) 832.
[3] I.W.C.E. Arends, P. Gamez, R.A. Sheldon, Adv. Inorg. Chem. 58 (2006) 235.
[4] S. Itoh, Curr. Opin. Chem. Biol. 10 (2006) 115.
[5] C. Belle, W. Rammal, J.L. Pierre, Inorg. Biochem. 99 (2005) 1929.
[6] R. Boulatov, Pure Appl. Chem. 76 (2004) 303.
[7] R.A. Himes, K.D. Karlin, Curr. Opin. Chem. Biol. 13 (2009) 119.
[8] K.D. Karlin, S. Itoh (Eds.), Copper-Oxygen Chemistry, John Wiley & Sons, 2011.
[9] H.S. Jung, P.S. Kwon, J.W. Lee, J.I. Kim, C.S. Hong, J.W. Kim, S. Yan, J.Y. Lee, J.H. Lee, T. Joo, J.S. Kim, J. Am. Chem. Soc. 131 (2009) 2008.
[10] Y. You, Y. Han, Y.M. Lee, S.Y. Park, W. Nam, S.J. Lippard, J. Am. Chem. Soc. 133 (2011) 11488.
[11] M. Verma, A.F. Chaudhry, M.T. Morgan, C.J. Fahrni, Org. Biomol. Chem. 8 (2010) 363.
[12] S.Y. Chung, S.W. Nam, J. Lim, S. Park, J. Yoon, J. Chem. Commun. (2009) 2866.
[13] K.P. Wainwright, Coord. Chem. Rev. 166 (1997) 35.
[14] P.V. Bernhardt, G.A. Lawrance, Coord. Chem. Rev. 104 (1990) 297.
[15] M. Roger, L.M.P. Lima, M. Frindel, C. Platas-Iglesias, J.-F. Gestin, R. Delgado, V. Patinec, R. Tripier, Inorg. Chem. 52 (2013) 5246.
[16] J.C. Timmons, T.J. Hubin, Coord. Chem. Rev. 254 (2010) 1661.
[17] M. Suchy, R.H.E. Hudson, Eur. J. Org. Chem. (2008) 4847.
[18] W. Han, Z.D. Wang, C.Z. Xie, Z.Q. Liu, S.P. Yan, D.Z. Liao, Z.H. Jiang, P. Cheng, J. Chem. Cryst. 34 (2004) 495.
[19] K. Wieghardt, E. Schoeffmann, B. Nuber, J. Weiss, Inorg. Chem. 25 (1986) 4877.
[20] I.A. Fallis, R.D. Farley, K.M.A. Malik, D.M. Murphy, H.J. Smith, J. Chem. Soc., Dalton Trans. (2000) 3632.
[21] CRYSALIS-CCD 170, Oxford-Diffraction, 2002.
[22] CRYSALIS-RED 170, Oxford-Diffraction, 2002.
[23] M. Sheldrick, SHELX97. Program for Crystal Structure Analysis, University of Gottingen, Gottingen, Germany, 1997.
[24] L.J. Farrugia, J. Appl. Crystallogr. 32 (1999) 837.
[25] M. Roger, V. Patinec, M. Bourgeois, R. Tripier, S. Triki, H. Handel, Tetrahedron 68 (2012) 5637.
[26] S.J. Brudenell, L. Spiccia, A.M. Bond, P. Comba, D.C.R. Hockless, Inorg. Chem. 37 (1998) 3705.
[27] O. Schlager, K. Wieghardt, B. Nuber, Inorg. Chem. 34 (1995) 6649.
[28] J.A. Halfen, S. Mahapatra, E.C. Wilkinson, A.J. Gengenbach, V.G. Young Jr., L. Que Jr., W.B. Tolman, J. Am. Chem. Soc 118 (1996) 763.
[29] L. Yang, W.B. Tolman, J. Biol. Inorg. Chem. 17 (2012) 285.
[30] N. Le Poul, M. Campion, B. Douziech, Y. Rondelez, L. Le Clainche, O. Reinaud, Y. Le Mest, J. Am. Chem. Soc. 129 (2007) 8801. and refs. cited.
[31] N. Menard, Y. Hériot, Y. Le Mest, O. Reinaud, N. Le Poul, B. Colasson, Chem. Eur. J. 19 (2013) 10611.
[32] Z. He, S.B. Colbra, D. Craig, Chem. Eur. J. 9 (2003) 116.
[33] E.R. Kay, D.A. Leigh, F. Zerbetto, Angew. Chem., Int. Ed. 46 (2007) 72.
[34] S.K. Sharma, G. Hundal, R. Gupta, Eur. J. Inorg. Chem. (2010) 631.
[35] B. Cervera, J.L. Sanz, M.J. Ibanez, G. Vila, F. Lloret, M. Julve, R. Ruiz, X. Ottenwaelder, A. Aukaulo, S. Poussereau, Y. Journaux, M.C. Munoz, J. Chem. Soc., Dalton Trans. (1998) 781.
[36] S.L. Jain, J.A. Crayston, D.T. Richens, J.D. Woolins, Inorg. Chem. Commun. 5 (2002) 853.
[37] Y. Dong, L.F. Lindoy, Coord. Chem. Rev. 245 (2003) 11.
[38] J.K. Clegg, D.B. Bray, K. Gloe, K. Gloe, M.J. Hayter, K.A. Jolliffe, G.A. Lawrance, G.V. Meehan, J.C. McMurtrie, L.F. Lindoy, M. Wenzel, Dalton Trans. (2007) 1719.